REVISTA MATÉRIA V.28 N.2
ISSN 1517-7076 articles e20230128, 2023

Influence of zinc sulphate in microstructure and strength properties of blended cementitious concrete system

Archana Murugan[1], Ramasamy Vasudevan[2]

[1]Dhirajlal Gandhi College of Technology, Department of Civil Engineering, 636309, Salem, Tamil Nadu, India.

[2]Adhiparasakthi Engineering College, Department of Civil Engineering, Melmaruvathur, 603319, Chengalpattu, Tamil Nadu, India.

e-mail: archanamurugan17@gmail.com, rams_apec@yahoo.co.in

ABSTRACT

In recent decades, greenhouse gas emission and global warming are the major threat to climatic change variability. The quality of concrete can be enhanced by the addition of a supplementary cementitious material to portland cement. In this study, fly ash is utilized as a supplemental cementitious material (SCM). The purpose of this research is to test and study the mechanical and thermal properties of blended concrete containing ordinary portland cement, fly ash and zinc sulphate as well as to investigate the microstructure in order to study the influence of zinc sulphate on the hydration process of concrete. This research mainly focused on the changes occurring in the strength, retarding mechanism, setting time, mineralogy, and microstructure caused by the addition of zinc sulphate in concrete. Ordinary portland cement, fly ash, pulverized fly ash and zinc sulphate are used in the blended concrete. The varied proportions of fly ash and zinc sulphate in the mix are 15%, 30%, 45%, and 60% respectively. The strength characteristics can be increased by fly ash pulverization. Hence the research focuses in exploring the addition of fly ash, pulverized fly ash and zinc sulphate anhydride to the concrete mix.

Keywords: Fly ash, Ordinary Portland Cement, Pulverized fly ash, Zinc sulphate.

1. INTRODUCTION

An emerging building sector Plain concrete (PC) is a main potential member for enhancing the structural performance. The major utilization of PC in the buildings are both structural and non-structural members. It is a well-known fact that the concrete industry contributes to a large amount of CO_2 emissions globally [1, 2]. In response to the rising alarm of climate changes and sustainable construction, several researchers attempted to partially replace sustainable waste into conventional building materials [3, 4] without compromising their mechanical properties and sustainability [5, 6]. Hypo sludge is a sustainable waste material produced from the paper mill and every year it requires a larger landfill space to dispose of [7]. Cement is one of the leading members for the concrete matrix and it is harmful to the environment [8]. Therefore, several studies have been investigated the partial replacement of hypo sludge into the portion of the cement concrete matrix with different ratios. It significantly increases the durability of concrete and minimizing the environmental impacts [9].

PC is remarkably known for high compressive strength, but is strongly prone to cracks and brittle, due to the tensile stress and such stress usually carried by steel reinforcement bars [10]. Traditionally, the advent of the addition of fibers as reinforcement into the PC can profoundly be increasing the tensile properties. Concrete causes up to 8% of global CO_2 emissions. In comparison, aviation accounts for about 2.8 percent of total global emissions, according to a 2020 report from the International Energy Agency. During the cement-making process, materials are heated at very high temperatures, requiring large amounts of energy – mostly powered by fossil fuels. Concrete is used to create hard surfaces which contribute to surface runoff that may cause soil erosion, water pollution and flooding. The inclusion of fibers in the concrete can improve the mechanical properties and acts as a barrier for the structural cracks and brittle failures, also it reduces the crack width and increases the propagation resistance [11]. Therefore, an extensive study has been carried out to enhance properties by the fiber inclusion. Commonly used fiber types are, steel fiber, glass fiber, synthetic fiber, such as carbon, acrylic, polyethylene terephthalate (PET), and natural fiber, such as coconut, sugarcane bagasse, jute, wood, palm, sisal, and basalt. These fibers are improving the physio-chemical properties of the concrete as a result of incorporating the fibers by volume fraction percentage, also it reduces the structural and shrinkage cracks [12].

Corresponding Author: Archana Murugan Received on 15/04/2023 Accepted on 17/05/2023

DOI: https://doi.org/10.1590/1517-7076-RMAT-2023-0128

Several researchers successfully employed adding the steel fiber in concrete to enhance the crack resistance, post cracking tensile strength, fire resistance, ductility, impact resistance, conductivity properties and energy absorption [13]. Chiefly, the fiber can hold the concrete matrix under the flexural loading condition even after a large carking width and the brittle concrete turns into a ductile matrix. However, many suggested negative sides of the steel fiber inclusion in the concrete. It can adversely affect the workability, compressive and flexural strength, and balling effects. Also, the corrosion of steel fiber can be significantly deteriorating the performance of concrete and much expansive than the PC [14]. On the other hand, glass fiber possesses excellent mechanical properties and it increases the tensile, flexural strengths and ductility in compression. However, it is susceptible to the alkaline environment of concrete and the hydration of cement destroys glass fiber [15]. Also, the higher PH level of concrete can cause the structures of glass fibers. Furthermore, many researchers have been attempted to study the inclusion of synthetic fibers into PC to enhance mechanical properties. The synthetic fibers are man-made products from polymers, which are harmful to the environment and it is prone to temperature effects [16, 17].

Several researchers reported that the addition of coconut fiber into the concrete can improve toughness while comparing to the other fibers [18]. On the other hand, Javad Torkaman et al. investigated the lightweight concrete block by the addition of wood fiber and it has low compatibility with the concrete matrix and higher moisture absorption in nature [19, 20]. WANG and CHOUW [21] has analysed the behaviour of coconut fibre reinforced concrete which gives better reality than the conventional result. Therefore natural fibers are getting major attention among the researcher due to their higher thermo physical and chemical properties and it is a sustainable material ALAVEZ RAMIREZ et al. [22]. Variations in fiber content, geometry, combination, distribution and orientation are all central contributors to making the structural design of Ultra High Performance Concrete [23]. TORKAMAN, ASORI and SADR MOMTAZI [24] determined The compressive strength of the concrete blocks due to the filler effect decreased with increasing cement replacement. However, the results show the effect of 25 wt% replacement of RHA and LPW with Portland cement do not exhibit a sudden brittle fracture even beyond the failure loads, indicates high energy absorption capacity, reduce the unit weight dramatically. Fibres are also one of the main reasons for the high unit cost and carbon footprint of Ultra High Performance Concrete. [25–27]. Consequently, increasing the knowledge on the effects of fibre reinforcement is an essential step towards the development of commonly accepted design codes and widespread use of Ultra High Performance Concrete [28].

In particular, the selection approaches of fiber material based on its geometry, thermos-physical properties, chemical compatibility in the concrete matrix, availability and cost. In recent years, basalt fiber getting renewed interest as a natural fiber and it is widely accepted to enhancing the mechanical properties of concrete. Basalt fiber is an eco-friendly material and it is produced by melting basalt rocks at 1450 °C as it is the least temperature. In general, basalt fiber well-known for its superior tensile strength, high temperature, and chemical resistance. Studies have shown that the inclusion of basalt fiber into the concrete matrix can improve the tensile and flexural strength, ductility in compression and also it controls the shrinkage crack [20]. Fly ash, ground nut shell ash and other renewables have been studied for partially replacing cement which have been successful. Even though the study about the fly ash has been done the chemical nature and the effects of usage of hard retarding admixtures are not been studied entirely. As the fly ash become a major replacement material and so the pulverized fly ash will soon become a key replacement material for cement in construction industry, thus this study involves in understanding the hydration behaviour, strength aspects and durability aspects of blended concrete with hard retarding compounds.

The current study investigates the inclusion of pulverized fly ash into concrete in order to improve the mechanical properties and long-term durability of the concrete. Additionally, the study examines both the mechanical and long-term durability properties of the blended concrete consisting of OPC, fly ash and zinc sulphate in order to investigate microstructure and to learn more about the influence of zinc sulphate on the hydration process of the concrete.

2. MATERIALS AND METHODS

2.1. Material

The primary binding material used in this project is Ordinary Portland Cement (OPC) 53 grade. Fly ash (FA) and zinc sulphate have been used to replace the OPC, which causes further environmental difficulties owing to its use. The fly ash utilized in this investigation is collected from the Ennore thermal power plant. The fly ash (FA) is classified as Class F as per codal provision. The pulverization process reduces the particle size of the fly ash and enhances the strength characteristics. Various fineness tests are carried out in order to demonstrate the decrease in particle size which is visible after the pulverization of fly ash, and the material is referred to as fine fly ash (FFA). The size of fine fly ash varies from 10–100 microns. However, the chemical nature of fly ash and

fine fly ash should remain unchanged throughout the pulverization process. The particle size reduction affects the fine fly ash material reactivity. River sand passing in 4.75 mm sieve size and stone aggregate retained in 10 mm sieve are utilized in this work [21, 22]. The fundamental properties of the fine and coarse aggregates are examined, and the results are in agreement with the IS 383. Zinc sulphate anhydrate is used as a retarder in the concrete as it is compatible with the different fly ash mixes used in the concrete. It is also used as an additive to concrete to act as a hardener, especially for use in floors. The properties of zinc sulphate is having the density of 3.54 g/cm^3. A trial-and-error method is used to determine the optimal zinc sulphate content with the mix percentages varying between 0.3 and 0.5%, 1%, 3%, 5%, and 7%. The optimum zinc sulphate content is determined by the compressive strength achieved after 7 days of normal curing.

2.2. METHODS

2.2.1. Analyzing the properties

Zinc sulphate is used mainly to neutralize new cement and plaster surfaces before they are painted or treated. It is also used as an additive to concrete to act as a hardener, especially for use in floors. Zinc sulphate is odorless and has a white powder appearance. Zinc sulphate is non-combustible and soluble in water. It emits toxic fumes of zinc oxide and sulphur oxides during decomposition. It is widely used in the prevention and treatment of zinc deficiency. FFA concrete has low early age strengths above 60% cement replacements. HVFA concrete has a higher sulphate/acid/chloride resistance and a lower shrinkage. Higher the fineness of fly ash and additives, greater the reactivity and hydration. Fine fly ash should be in the size ranges from 10–100 microns. The specific gravity of fly ash ranges from a low value of 1.90 for a sub-bituminous ash to a high value of 2.96 for an iron-rich bituminous ash (Figure 1).

2.2.2. Mix design and experimental program

The concrete cube specimens of the size 10 × 10 × 10 cm are casted for all the concrete mixes ranging between 15% to 60% fly ash and fine fly replacement in concrete. The cylinders of diameter 10 cm and height 20 cm and prisms of size 10 × 10 × 50 cm are casted and tested. Three cube specimens are cast to assess strength of mix at 7, 14, 28 and 56 days correspondingly. The OPC is substituted by fly ash with 15%, 30%, 45%, and 60% where specimens are evaluated for mechanical strength and optimal proportion of fly ash was identified. The addition of cement with fly ash and ZnS is done depending on its proportion to cement weight. The concrete specimens are prepared for a total of 24 mix combinations. The replacements are done for the cement by fly ash and pulverized fly ash at varying OPC 53 Grade range from 15 to 60% at the addition of 15%. Based on the mix design calculations the summary of mix proportions for various mix concrete and mix proportions were optimized according to the specific gravity of the cementitious materials which are used in

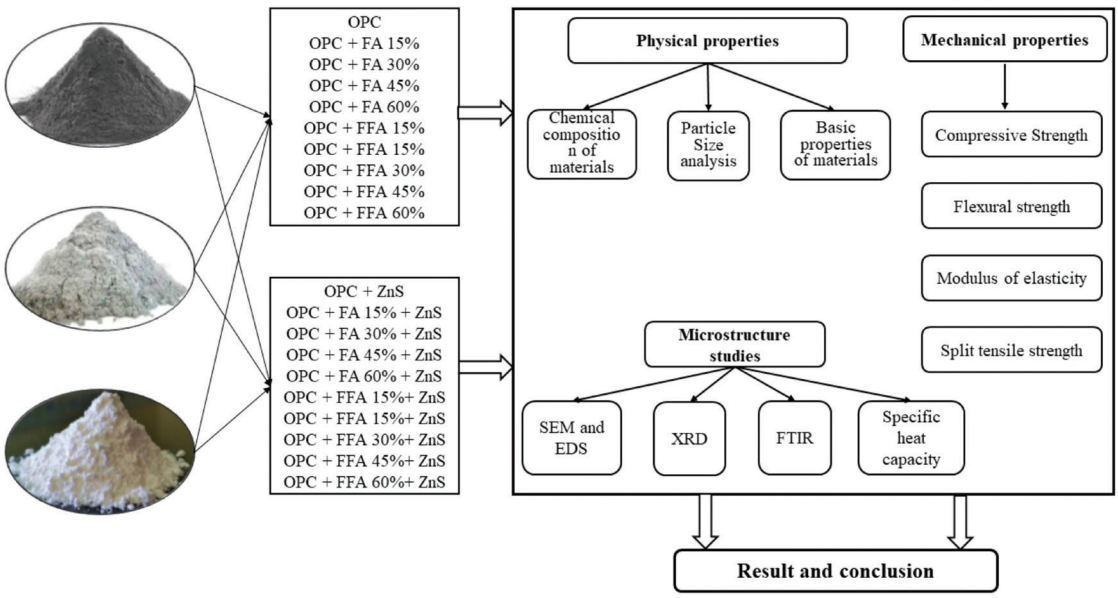

Figure 1: Methodology of the present research study.

this study for the preparation of concrete. The M40 grade of concrete mix proportions are having the ratio is 1:1.508:1.85, cement content is 520 kg/m^3, coarse aggregate is 960.284 kg/m^3, fine aggregate is 784.252 kg/m^3, Water is 208 l/m^3 are used [23].

2.2.3. Concrete specimen preparation and testing

In accordance with IS 4031 standards, the physical and chemical characteristics of materials are evaluated and characterized. The concrete cube specimens are casted in a 100 mm and tested in accordance with IS 516. Tests on the compressive strength of concrete specimens are carried out after 7, 14, 28 and 56 days using the SERVO FCT-EC-1000 compression testing machine (CTM). Specimens of 100 mm × 200 mm are casted and tested in CTM for the purpose of determining the tensile strength of the concrete mix. During the application of load, the cylinder is put along its length and then the load is delivered across the length of the cylinder. The flexural strength of the concrete mix is determined by testing prism with the following dimension: 100 mm × 100 mm × 500 mm in accordance to ASTM standard [24].

2.2.4. Fineness of cementitious particles

The fineness of fine powder materials is assessed by specific surface area and retained weight sieve. Fineness is determined using Particle size analyzer, Blaine fineness and Sieve residue. The particle size distribution is determined for the material under various pulverization conditions ranging from 15 minutes to 120 hours. The particle size is measured using the CilasEcosizer Dry Equipment in accordance to ASTME 2651-13 standard. When particles are placed in a row, the Blaine value is an indicator of the particular surface area that is defined by the dispersion of particles across the region and the value is expressed in terms of m^2/kg. Finding of fineness modulus through sieve residue follows a very simple and standard procedure in which the cement material is sieved on IS sieve and the retained weight in the 90-micron IS sieve is calculated which provides the approximate identity for the residue [25].

2.2.5. Microstructural analysis

The powdered samples are subjected to SEM, EDS, XRD and FTIR analysis as part of the microstructural investigation of the concrete. FEI QUANTA 200, a high-resolution field emission scanning electron microscope is used to produce the SEM picture of the concrete specimen which produces the thickness of the concrete structure. In addition, the EDS data is collected using an EDAX 102 mm Octane Prime EDS Detector. During the bombardment of electrons with the sample, the Energy Dispersive X-Ray Spectroscopy (EDS) method is used to collect information about the chemical composition and the structural integrity. In order to determine the phase of the crystalline components X-Ray Powder Diffraction is utilized in which a 3-dimensional diffraction grating is produced by directing X-ray at the specimen. In order to get the diffraction pattern of the samples an X' Pert Powder XRD system with a 2θ range of 0–150° and Cu-K radiation is used to test the material. There is a variance in the peaks of the samples as a result of various mix combinations being used [26].

It is necessary to do an FTIR analysis in order to acquire a more thorough bond characteristic. There is a total of 500–7500 cm^{-1} of wavelength range covered by the equipment utilized for this test, which is a Bruker Alpha T. Radiation testing is performed on the samples using incident Kapton radiation ranging from 115 to 150 A. A Differential Scanning Calorimeter (Netzsch - Germany) with the following specifications is used to test the powdered concrete sample: heating and cooling rates ranging from 0.001 °Celsius per minute to 500 °Celsius per minute, and temperature accuracy of 0.1 °Celsius per minute. The test is performed at a medium heating rate of 10 °Celsius per minute and an operating temperature of –20 °C to 120 °C. Individual sample specific heat capacities must be finalized by making necessary adjustments to the reference sample (sapphire).

3. RESULTS AND DISCUSSION

3.1. Chemical composition of materials

The chemical composition of the materials as shown in Table 1 reveals that the availability of CaO is high in cement while the SiO_2 content is high in the fly ash which infers that the formation of CSH will be more in the fly ash mix specimen. It is inferred that pulverizing fly ash reduces the size of particle but does not affect its chemical properties. In addition to the CSH structure the other crystalline structure that increases the specimen strength is mullite, the composition indicates that the amount of Al_2O_3 is also high in fly ash, thus there will be more mullite in concrete [27].

The specific gravity of cement is 3.13 g/cc, 2.88 g/cc for fly ash, 2.98 g/cc for fine fly ash which indicates that the cement possesses higher specific gravity value than other materials and so it can be inferred that cement

Table 1: Comparison of chemical composition.

Materials	SiO_2	Al_2O_3	Fe_2O_3	CaO	MgO	K_2O	Na_2O	SO_3	LOI
OPC	23.31	6.54	4.37	58.32	1.23	0	0	2.13	1.55
FA	55.9	24.90	7.84	2.12	1.64	1.35	1.06	0.69	2.27
FFA	55.31	25.13	7.46	2.59	1.58	1.37	1.04	0.7	2.14

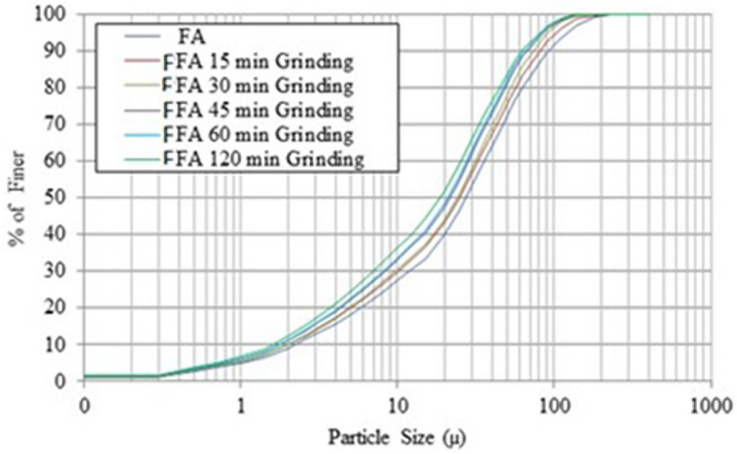

Figure 2: Particle size analyzer of grinded fly ash materials.

has higher density, while compared to all other materials. Besides the finer cementitious particles, the sand and coarse aggregates are also tested for specific gravity and the specific gravity value is obtained as 2.61 g/cc and 2.95 g/cc respectively [28, 29]. Fineness Modulus of the fine aggregate is 2.256 mm and most of the particles of aggregates are fine and retained between the sieve sizes of 0.6 to 0.15. The fineness modulus of coarse aggregate is 6.04 and it can be observed that most of the aggregate lies between 12.5 mm and 10 mm sieve.

3.2. Particle size analysis

The particle size analyzer result represented in Figure 2 indicates that the particle size of pulverized fly ash ranges from micro to Nano in its particle distribution and the percentage of finer particle increases with grinding time. By considering the economical and optimistic pulverization time 120 minutes ball milled fly ash is used for the concrete preparation and further tests [30, 31]. The Blaine fineness value of the fine raw cementitious materials indicates that the fineness value 331 m^2/kg of OPC is higher than the fly ash fineness value of 264 m^2/kg and fine fly ash has the highest Blaine fineness value of 608.44 m^2/kg. The sieve residue is a simple yet an effective way to indicate the fineness of the cementitious particles. This test proves that the fine fly ash particles are very fine with fineness modulus of 1.8% whereas OPC and fly ash have 5% and 5.39% fineness modulus respectively [32].

3.3. Basic properties of materials

The quantity of water required to achieve the desired consistency increases as the amount of fly ash in cement mix grows according to the consistency test result. A normal consistency of 27% is attained for ordinary Portland cement mix. Fine fly ash when used as a substitute material reduces the amount of water required compared to the fly ash mix [33]. The initial and final setting time for varied amounts of ZnS is depicted in Figure 3. It can be observed that the rise in the quantity of ZnS increases the setting time correspondingly. The setting time of the specimen is enhanced 50% on the addition of ZnS to the concrete mix which demonstrates that zinc sulphate may be utilized as a concrete retarder [34]. The retarding impact of ZnS in concrete may be minimized by lowering the proportion of ZnS in the concrete.

The formation of a transient compound in the concrete, which is caused by the addition of ZnS, is the root cause of the concrete's retarding action. Because of the good retarding effect of zinc sulphate in concrete and other construction materials, further research into the strength and other aspects of zinc sulphate blended concrete composites is needed. The results of this study show that zinc sulphate can be used as a possible retarder

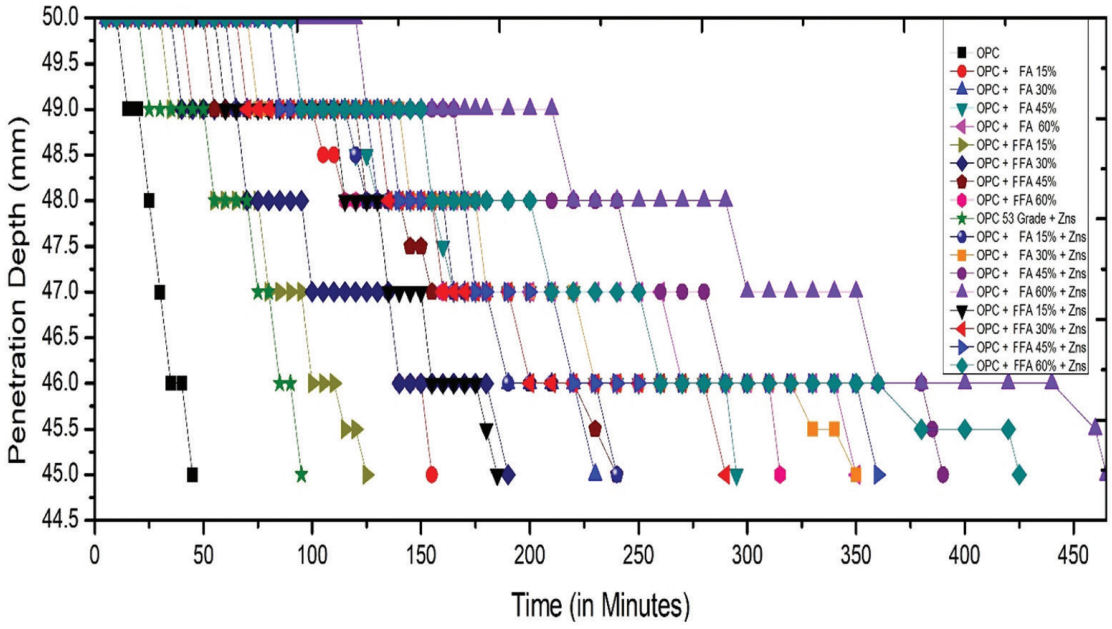

Figure 3: Setting time of blended mix proportions.

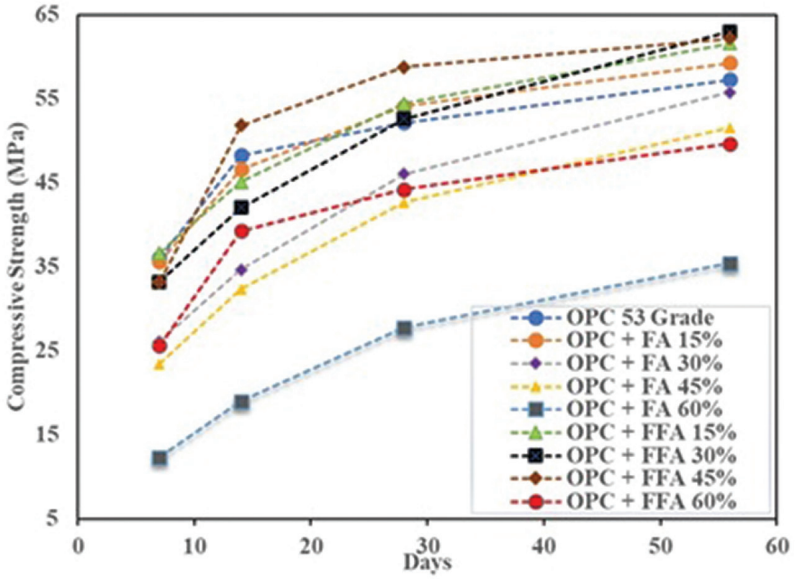

Figure 4: Compressive strength of blended concrete without ZnS.

in concrete and other construction materials. The crushing value of aggregate is 8.53%, the maximum crushing value of aggregate should be less 30% according to IS 2386 – Part 4. This is evident that the tested aggregate is very good in withstanding the crushing load. The aggregate impact value is 14.2% which is good according to IS 2386 – Part 4. Thus, these results show that the aggregates are very much qualified and strong enough to withstand higher load [35].

3.4. Compressive strength of fly ash blended concrete

The compressive strength of specimen is shown in Figure 4 and Figure 5. From the result it can be inferred that the strength of concrete specimen containing fine fly ash is significantly high than the strength of concrete specimen without fly ash. In this research much strength is produced by the concrete specimen with 60% fine fly ash replacement which is closer to the 30% fly ash replacement which infers that pulverization increases the strength characteristics [36, 37]. There is no significant impact on the strength of the concrete containing fly ash

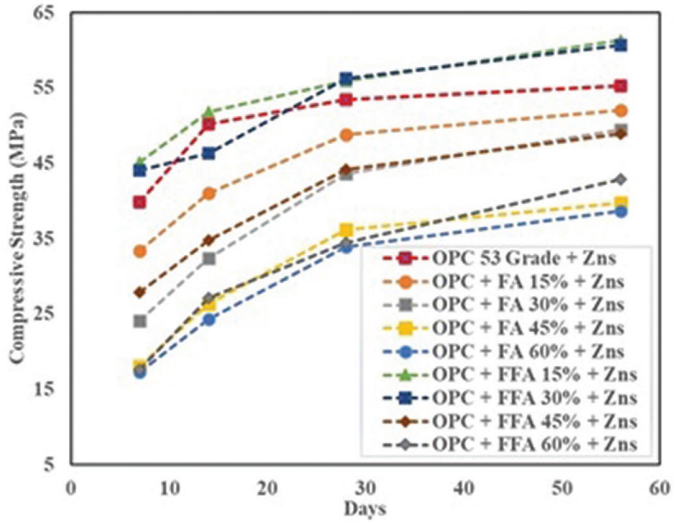

Figure 5: Compressive strength of blended concrete with ZnS.

upon the addition of zinc sulphate but when used in proportions greater than 60% it deters the setting of concrete specimen. From the compressive strength it can be inferred that 15% fly ash and 45% fine fly ash addition is the optimal mix and the chemical properties of the concrete can be studied.

3.5. Split tensile strength of fly ash blended concrete

The comparison of split tensile strength of the concrete specimens are explained. It demonstrates that the concrete tensile strength is significantly lower than its compressive strength. The test is carried out in accordance with IS 5816. It demonstrates that the 60% substitution of fly ash resulted in a significantly lower tensile strength in comparison to the whole mix. While 60% replacement of fine fly ash indicates a strength that is very close to the 45% replacement of fly ash, the 45% replacement of fly ash indicates a strength that is far lower. The strength of 45% fine fly ash replacement was also found to be much greater in this case. It can be observed in Figure 6 that the cylinder splits along the diameter of the concrete specimen, which is consistent with previous findings. By taking the maximum load that is delivered to the specimen and dividing it into equal halves, the specimen is divided in half. According to the preceding discussion, using the load value in the equation converts the load into split tensile strength of concrete [38].

3.6. Flexural strength of fly ash blended concrete

The specimen tested during the flexural strength test reveals that the failure of the specimen occurred in the centre of the specimen throughout its length. A minor loss in flexural strength is noticed with an increase in the replacement of fly ash in concrete, which is consistent with previous findings. The findings reveal that the addition of fly ash to the concrete at a rate of 15% has boosted the flexural strength of the mixture [39].

With reference to Table 2 which depicts the changes in flexural strength, it can be concluded that the fine fly ash has supplied significantly better flexural strength. Concrete's strength increased by 6.25% when 45% FFA was substituted for cement in the mix, which represents a significant improvement in terms of both strength gain and replacement of cement. The addition of 15% FFA to the mix has raised the compressive strength of the concrete by 25% compared to the original OPC mix. Furthermore, the strength characteristics of the specimens followed a very similar pattern to those of the compressive strength of the specimens.

3.7. Modulus of elasticity

Based on the compressive and split tensile strengths of the fly ash blended concrete, the optimal fly ash replacements for cement in concrete are determined to be 15% fly ash and 45% fine fly ash replacements for cement in concrete, respectively. The modulus of elasticity of the specimens is computed based on the values of stress and strain in the specimens. The E value of a specimen is computed by taking the slope of stress and strain at the point where elasticity terminates and dividing it by the number of stresses and strains. This modulus of elasticity reveals the capacity of concrete to tolerate strain and stress when subjected to different loads. Figure 7 compares the E value of the fly ash blends and indicates that the value is higher for the 45% FFA replaced concrete.

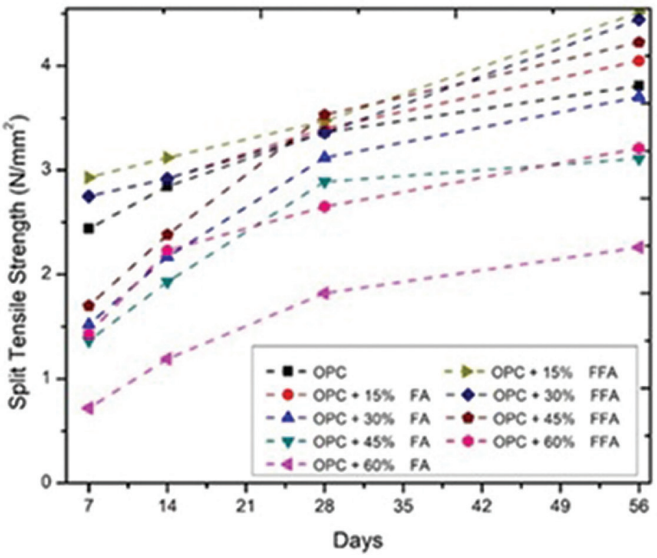

Figure 6: Split tensile strength comparison for different mix.

Table 2: Comparison of flexural strength of concrete.

MIX COMBINATION	ULTIMATE LOAD (KN)	FLEXURAL STRENGTH (MPa)
OPC	16	8
OPC + 15% FA	18	9
OPC + 30% FA	16	8
OPC + 45% FA	15	7.5
OPC + 60% FA	11	5.5
OPC + 15% FFA	20	10
OPC + 30% FFA	19	9.5
OPC + 45% FFA	17	8.5
OPC + 60% FFA	14	7

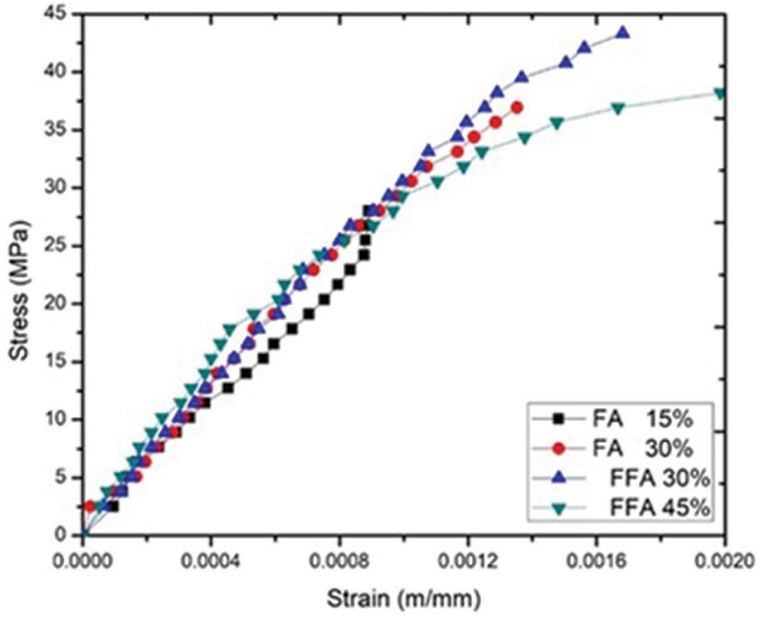

Figure 7: Comparison of stress strain of optimum fly ash concrete blends.

It is discovered that 15% FA replaced concrete has a larger modulus of elasticity when compared to the other three mixes. This is due to the increased strength in the concrete blend used in making the 15% FA replaced concrete. However, when comparing peak load or peak stress, 30% FFA mixes are able to tolerate far more stress than any of the other blends combined and the stress strain variations of the concrete specimen which illustrates that all of the specimens have stress strain variations that are almost identical to one another, and that the specimen failure occurs sooner for the 15% fly ash substituted concrete. While compared to 15% and 30% replacement, 30% replaced concrete has shown stronger stress withstanding capabilities than the other two percentages. However, the concrete that was substituted with 30% fine fly ash was able to tolerate much greater stress than all other concrete specimens. FFA blended concrete has superior strain withstanding capability when considering strain withstanding capability when considering strain withstanding capability [40]. This once again demonstrates the efficiency of FFA blended concrete as a construction material. This fine fly ash substituted concrete, as a result, has the potential to be employed as a viable replacement material for cement in concrete construction. Figure 7 illustrates the failure of specimen over their whole length indicating that they have collapsed along their entire circumference and in addition to the failing specimen it also shows the deflectometer connected to it.

3.8. Microstructure studies

3.8.1. SEM and EDS

SEM and EDS images of the specimen and the SEM images at a magnification of 5 microns is compared. SEM images of fly ash and fine fly ash reveal size differences between the particles of fly ash and fine fly. The shape of fly ash particles is round whereas it is highly irregular in shape for fine fly ash and the fine fly ash is small in comparison to the fly ash [41, 42]. The comparison of the FA and FFA concrete reveals that the FA concrete contains a significant amount of un-hydrated SiO_2 in the structure, which can be identified by the spherical structure in the SEM images, whereas the FFA concrete contains no un-hydrated compounds, demonstrating that pulverization increases the reactivity between the water and cementitious products, resulting in a very compact structural formation (Figure 8). Additionally, as compared to normal concrete specimens, the FFA concrete exhibits a highly compact structure. The presence of needle-like structures in the concrete can clearly be seen when comparing images of concrete with and without zinc sulphate indicating that ettringite has formed as a result of zinc sulphate exposure. Crystal formation in concrete is conceivable and the majority of the structure is derived from SiO_2, CSH, and mullite. This also demonstrates the improvement in concrete strength that has occurred as a result of the inclusion of FFA [43]. According to the EDS graphs, the addition of ZnS has no effect on the elemental range of the concrete, which is consistent with the results of previous studies. The elemental analysis of FA and FFA reveals a similar pattern, indicating the presence of components of a comparable sort. This verifies that the chemical characteristics of fly ash were not significantly altered throughout the pulverization process, as previously reported.

When comparing the SEM images of 60% fly ash replaced concrete and 60% fine fly ash replaced concrete, it can be noticed that the fine fly ash replaced concrete has a more enhanced and compact structure than the 60% fly ash replaced concrete. It is clear that more hydration is taking place in the concrete; additionally, the 60% fly ash replaced concrete exhibits more un-hydrated products, which is the result of more SiO_2 in its system and less CaO to form the hydrated compounds that are required for the formation of crystalline compounds and ultimately for the provision of strength.

3.8.2. XRD

Figure 9 depicts the diffraction pattern of the FA and the FFA, respectively. According to this, the presence of quartz and mullite in raw materials is responsible for the majority of the peaks; moreover, when comparing the peak at 26.6 with the peak at 26.6, the peak extends to a greater intensity for FFA, which is ascribed to quartz. Additionally, for FA, a tiny peak for Fe_2O_3 is found around 33.25 °C. There is no difference between the FFA and FA samples in terms of the diffraction patterns they produce, except from these modifications [44].

The primary peak of OPC and 15% FA blended concrete differs in terms of counts when compared to each other, indicating that the C-S-H compound is more readily accessible in 15% FA blended concrete. When compared to traditional concrete, this resulted in a significant improvement in the strength of the finished product. Additionally, when comparing the 45% FFA mixed concrete to the other blends, the elongation of the primary peak is much greater. C-S-H is responsible for the majority of the peak values in the OPC + 45% FFA mixed concrete. Analysis using zinc sulphate discovered that ettringite was present in some of the peaks. Ettringite development is related to the presence of sulphate in the concrete during the curing process.

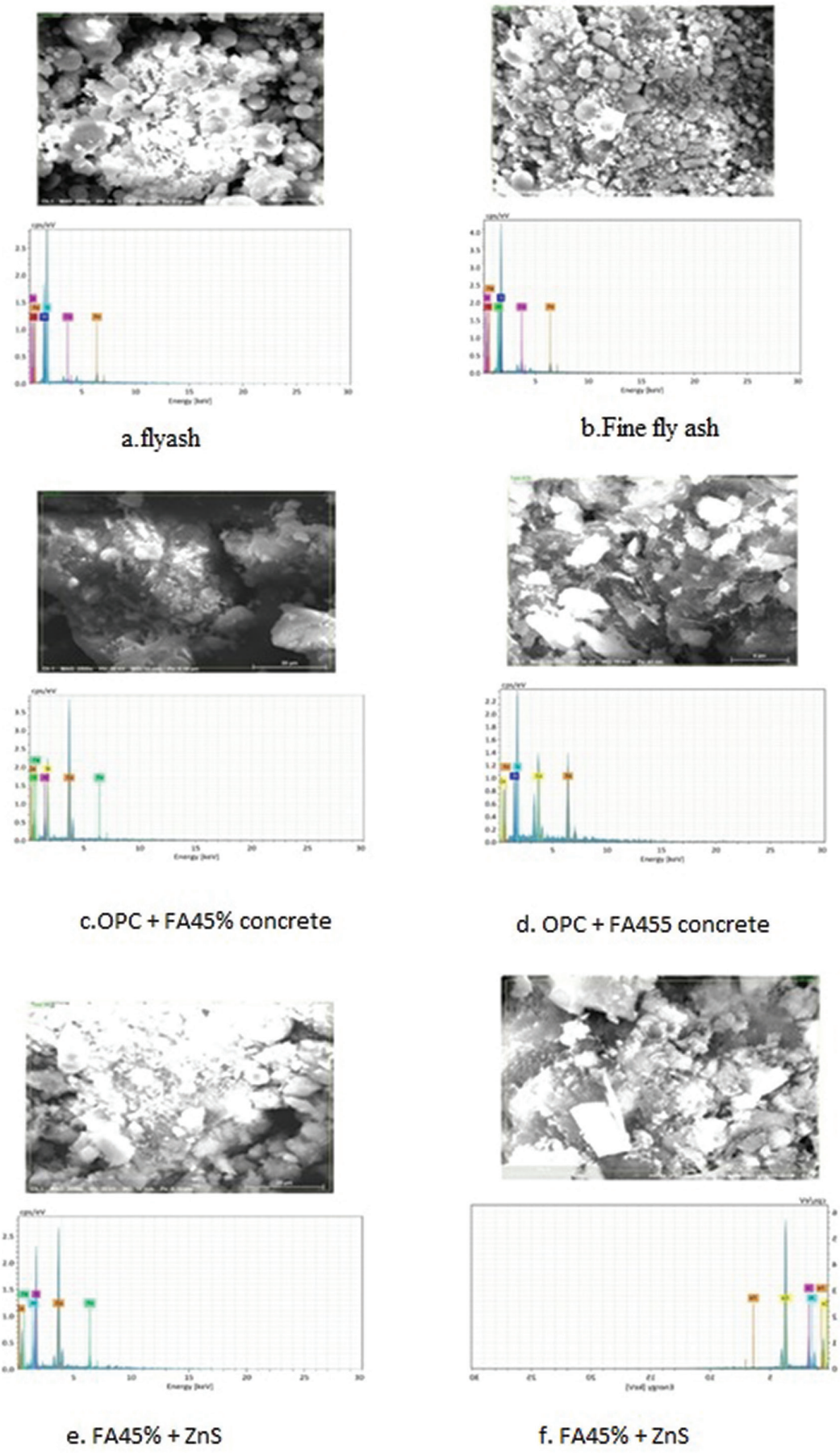

Figure 8: Comparison of SEM images and EDS results of samples.

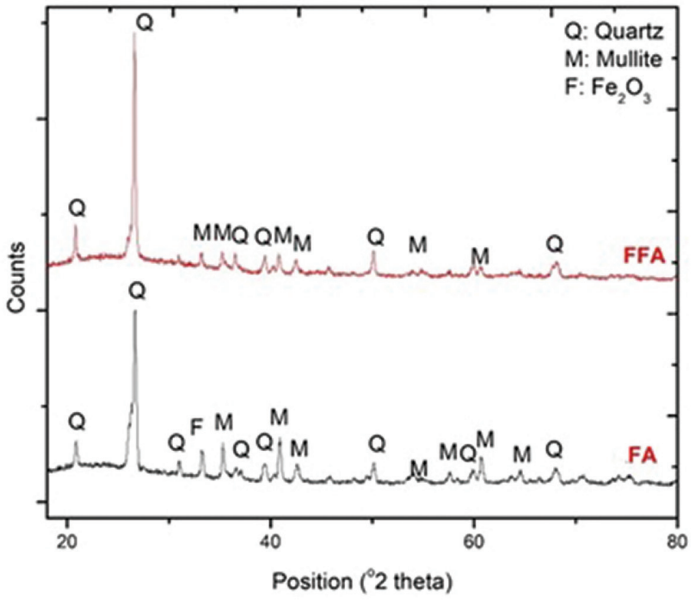

Figure 9: XRD analysis of fly ash and fine fly ash.

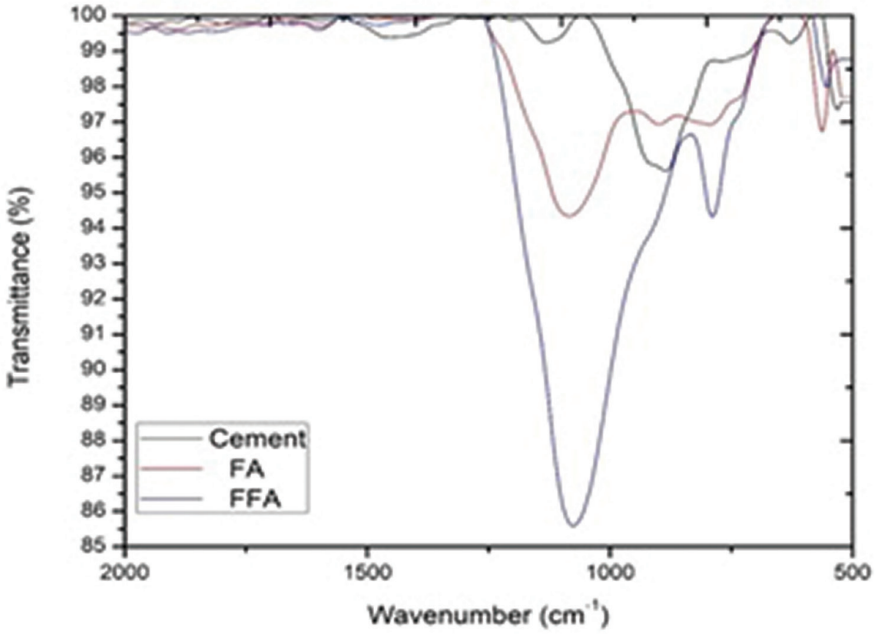

Figure 10: Comparison of FTIR results of raw materials.

In addition to ettringite, there is an abundance of $CaZn_2(OH)_6.2H_2O$ in peaks at 32.092 and the following equation describes the process by which calcium zincate is produced.

$$Zn(OH)_4^{2-} + Ca^{2+} + H_2O \rightarrow (CaZn(OH)_3)_2 \cdot 2H_2O + 2OH^-$$

The addition of ZnS decreased the production of C-S-H gel but increased the production of additional ettringite and the uncommon $CaZn_2(OH)6.2H_2O$ compound in its structure, according to XRD examination.

3.8.3. FTIR

The FTIR result of raw materials is depicted in Figure 10. The wavenumbers and their associated assignments are found in the literature. The broad waves for cement are present at 576–671 cm^{-1}, 790–1060 cm^{-1}, 1064–1196 cm^{-1} and 1313–1554 cm^{-1} range. The FTIR result for various mix containing zinc is represented in Figure 11.

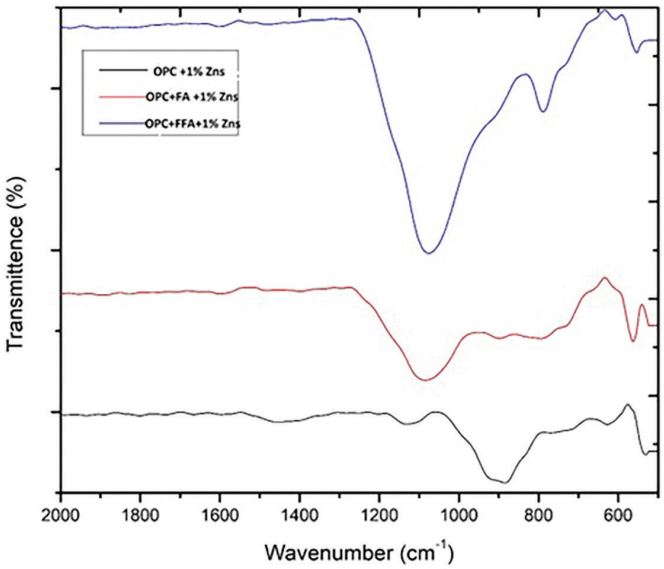

Figure 11: Comparison of FTIR results of 45% FFA blended concrete with and without ZnS.

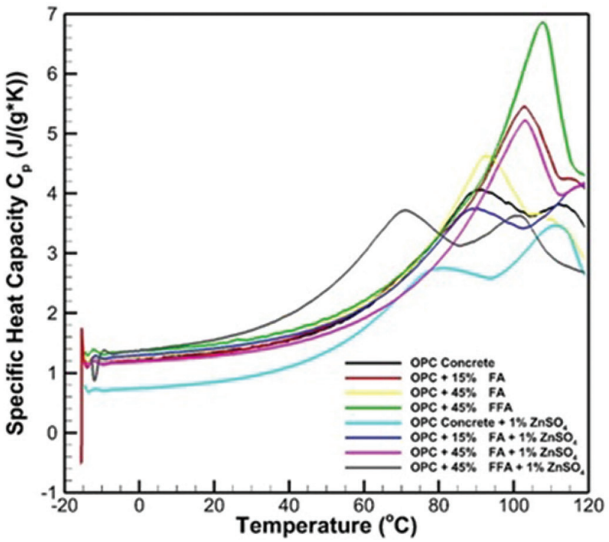

Figure 12: Specific heat capacity of specimen.

The Ettringite production is noticed in the specimen containing ZnS while there is a decrease in CSH gel production which explains lower strength in the specimen containing ZnS. The 45% FFA specimen consists more hydrated products which validates the XRD finding [45].

3.8.4. Specific heat capacity

The variation of specific heat capacity of the specimens with temperature is compared in Figure 12. The comparison is made between the specific heat capacity of OPC concrete, 15% fly ash replaced concrete, 45% fly ash concrete and 45% FFA concrete. As with increase in the fly ash content the heat storage ability of concrete has increased [46, 47]. By comparing 45% FA and FFA replacements the FFA indicate that the Cp increases with pulverization and the FFA concrete specimen performs poorly when compared to normal concrete.

4. CONCLUSIONS

The fly ash and fine fly ash replacement of 15% and 45% is deemed optimal. Due to compressive strength, setting time and alkali silicate reaction in concrete the ZnS content is optimized as 1%. With the addition of ZnS

the compressive strength of the fly ash blended concrete lowered while the initial strength of the concrete was increased. In addition to the strength and setting time characteristics, XRD analysis revealed that the concrete samples containing ZnS formed more ettringite and calcium zincate [$CaZn_2(OH)6.2H_2O$].

- In concrete containing ZnS the FTIR spectrum revealed decrease in formation of C-S-H and increase in ettringite formation which is verified by SEM images.
- The DSC findings demonstrate that adding fly ash to concrete enhances its heat storage capacity proportionately with FFA because it has a greater Cp.
- The addition of fine fly ash to concrete inhibits the creation of voids in the concrete, which reduces chloride penetration. As a result, the use of fine fly ash instead of cement enhanced all of the physical and microstructural qualities of concrete except the thermal properties which suggests that fine fly ash can be used in concrete as a substitute for cement.
- When analyzing the impacts of ZnS in concrete it has been discovered that it has an excellent concrete retarding effect.

As a result, it may be utilized as a possible retarder in concrete with a maximum permissible cement concentration of 1%. The impact of zinc sulphate on other regularly used secondary cementitious materials such as silica fume and GGBFS will be the focus of future research directions. Since pulverized fly ash is still considered as a research area further study is required to increase pulverization efficiency and to investigate the impact of additional chemical additives and admixtures.

5. BIBLIOGRAPHY

[1] JOSHI, S., GOYAL, S., SUDHAKARA REDDY, M., "Influence of biogenic treatment in improving the durability properties of waste amended concrete: a review", *Construction & Building Materials*, v. 263, pp. 120170, 2020. doi: http://dx.doi.org/10.1016/j.conbuildmat.2020.120170

[2] WU, H., LIN, X., ZHOU, A., "A review of mechanical properties of fibre reinforced concrete at elevated temperatures", *Cement and Concrete Research*, v. 135, pp. 106117, 2020. doi: http://dx.doi.org/10.1016/j.cemconres.2020.106117

[3] ALI, B., QURESHI, L.A., SHAH, S.H.A., *et al*., "A step towards durable, ductile and sustainable concrete: Simultaneous incorporation of recycled aggregates, glass fiber and fly ash", *Construction & Building Materials*, v. 251, pp. 118980, 2020. doi: http://dx.doi.org/10.1016/j.conbuildmat.2020.118980

[4] AHMAD, M.R., CHEN, B., YU, J., "A comprehensive study of basalt fiber reinforced magnesium phosphate cement incorporating fine fly ash", *Composites. Part B, Engineering*, v. 168, pp. 204–217, 2019. doi: http://dx.doi.org/10.1016/j.compositesb.2018.12.065

[5] COSTA, F.B.P.D., RIGHI, D.P., GRAEFF, A.G., *et al*., "Experimental study of some durability properties of ECC with a more environmentally sustainable rice husk ash and high tenacity polypropylene fibers", *Construction & Building Materials*, v. 213, pp. 505–513, 2019. doi: http://dx.doi.org/10.1016/j.conbuildmat.2019.04.092

[6] PUNURAI, W., KROEHONG, W., SAPTAMONGKOL, A., *et al*., "Mechanical properties, microstructure and drying shrinkage of hybrid fly ash-basalt fiber geopolymer paste", *Construction & Building Materials*, v. 186, pp. 62–70, 2018. doi: http://dx.doi.org/10.1016/j.conbuildmat.2018.07.115.

[7] SARADAR, A., NEMATI, P., PASKIABI, A.S., *et al*., "Prediction of mechanical properties of lightweight basalt fiber reinforced concrete containing silica fume and fly ash: Experimental and numerical assessment", *Journal of Building Engineering*, v. 32, pp. 101732, 2020. doi: http://dx.doi.org/10.1016/j.jobe.2020.101732

[8] GOEL, G., KALAMDHAD, A.S., "An investigation on use of paper mill sludge in brick manufacturing", *Construction & Building Materials*, v. 148, pp. 334–343, 2017. doi: http://dx.doi.org/10.1016/j.conbuildmat.2017.05.087

[9] GEDAM, B.A., BHANDARI, N.M., UPADHYAY, A., "Influence of supplementary cementitious materials on shrinkage, creep, and durability of high-performance concrete", *Journal of Materials in Civil Engineering*, v. 28, n. 4, pp. 1–11, 2016. doi: http://dx.doi.org/10.1061/(ASCE)MT.1943-5533.0001462

[10] FAVA, G., RUELLO, M.L., CORINALDESI, V., "Paper mill sludge ash as supplementary cementitious material", *Journal of Materials in Civil Engineering*, v. 23, n. 6, pp. 772–776, 2011. doi: http://dx.doi.org/10.1061/(ASCE)MT.1943-5533.0000218

[11] KUMAR, V.V.P., PRASAD, D.R., "Influence of supplementary cementitious materials on strength and durability characteristics of concrete", *Advances in Concrete Construction*, v. 7, n. 2, pp. 75–85, 2019. doi: https://doi.org/10.12989/acc.2019.7.2.075

[12] JUENGER, M.C.G., SIDDIQUE, R., "Recent advances in understanding the role of supplementary cementitious materials in concrete", *Cement and Concrete Research*, v. 78, pp. 71–80, 2015. doi: http://dx.doi.org/10.1016/j.cemconres.2015.03.018

[13] BRANSTON, J., DAS, S., KENNO, S.Y., *et al*., "Mechanical behaviour of basalt fibre reinforced concrete", *Construction & Building Materials*, v. 124, pp. 878–886, 2016. doi: http://dx.doi.org/10.1016/j.conbuildmat.2016.08.009

[14] PUJADAS, P., BLANCO, A., CAVALARO, S., *et al*., "Fibre distribution in macro-plastic fibre reinforced concrete slab-panels", *Construction & Building Materials*, v. 64, pp. 496–503, 2014. doi: http://dx.doi.org/10.1016/j.conbuildmat.2014.04.067

[15] TASSEW, S.T., LUBELL, A.S., "Mechanical properties of glass fiber reinforced ceramic concrete", *Construction & Building Materials*, v. 51, pp. 215–224, 2014. doi: http://dx.doi.org/10.1016/j.conbuildmat.2013.10.046

[16] LIU, B., GUO, J., ZHOU, J., *et al*. The mechanical properties and microstructure of carbon fibers reinforced coral concrete", *Construction and Building Materials*, v. 249, pp. 118771, 2020. doi: https://doi.org/10.1016/j.conbuildmat.2020.118771

[17] WANG, W., CHOUW, N., "The behaviour of coconut fibre reinforced concrete (CFRC) under impact loading", *Construction & Building Materials*, v. 134, pp. 452–461, 2017. doi: http://dx.doi.org/10.1016/j.conbuildmat.2016.12.092

[18] SAPPAKITTIPAKORN, M., SUKONTASUKKUL, P., HIGASHIYAMA, H., *et al*., "Properties of hooked end steel fiber reinforced acrylic modified concrete", *Construction & Building Materials*, v. 186, pp. 1247–1255, 2018. doi: http://dx.doi.org/10.1016/j.conbuildmat.2018.08.055

[19] MEZA DE LUNA, A., SHAIKH, F.U.A., "Anisotropy and bond behaviour of recycled Polyethylene terephthalate (PET) fibre as concrete reinforcement", *Construction & Building Materials*, v. 265, pp. 120331, Dec. 2020. doi: http://dx.doi.org/10.1016/j.conbuildmat.2020.120331

[20] X. Li, Y. Zhang, C. Shi, X. Chen, "Experimental and numerical study on tensile strength and failure pattern of high performance steel fiber reinforced concrete under dynamic splitting tension," Constr. Build. Mater, v. 259, pp. 119796, Oct. 2020. doi: https://doi.org/10.1016/j.conbuildmat.2020.119796

[21] WANG, W., CHOUW, N., "The behaviour of coconut fibre reinforced concrete (CFRC) under impact loading", *Construction & Building Materials*, v. 134, pp. 452–461, 2016. doi: http://dx.doi.org/10.1016/j.conbuildmat.2016.12.092

[22] ALAVÉZ-RAMÍREZ, R., MONTES-GARCÍA, P., MARTÍNEZ-REYES, J., *et al*., "The use of sugarcane bagasse ash and lime to improve the durability and mechanical properties of compacted soil blocks", *Construction & Building Materials*, v. 34, pp. 296–305, 2012. doi: http://dx.doi.org/10.1016/j.conbuildmat.2012.02.072

[23] SULTANA, N., HOSSAIN, S.M.Z., ALAM, M.S., *et al*., "An experimental investigation and modeling approach of response suFAce methodology coupled with crow search algorithm for optimizing the properties of jute fiber reinforced concrete", *Construction & Building Materials*, v. 243, pp. 118216, 2020. doi: http://dx.doi.org/10.1016/j.conbuildmat.2020.118216

[24] TORKAMAN, J., ASHORI, A., SADR MOMTAZI, A., "Using wood fiber waste, rice husk ash, and limestone powder waste as cement replacement materials for lightweight concrete blocks", *Construction & Building Materials*, v. 50, pp. 432–436, 2014. doi: http://dx.doi.org/10.1016/j.conbuildmat.2013.09.044

[25] OZERKAN, N.G., AHSAN, B., MANSOUR, S., *et al*., "Mechanical performance and durability of treated palm fiber reinforced mortars", *International Journal of Sustainable Built Environment*, v. 2, n. 2, pp. 131–142, 2013. doi: https://doi.org/10.1016/j.ijsbe.2014.04.002

[26] SABARISH, K.V., PAUL, P., BHUVANESHWARI, J., *et al*., "An experimental investigation on properties of sisal fiber used in the concrete", *Materials Today: Proceedings*, v. 22, n. Pt 3, pp. 439–443, 2019. doi: https://doi.org/10.1016/j.matpr.2019.07.686

[27] KIRTHIKA, S.K., SINGH, S.K., "Experimental investigations on basalt fibre-reinforced concrete", *Journal of The Institution of Engineers (India): Series A*, v. 99, n. 4, pp. 661–670, 2018. doi: http://dx.doi.org/10.1007/s40030-018-0325-4

[28] LARSEN, I.L., THORSTENSEN, R.T., "The influence of steel fibres on compressive and tensile strength of ultra high performance concrete: a review", *Construction & Building Materials*, v. 256, pp. 119459, 2020. doi: http://dx.doi.org/10.1016/j.conbuildmat.2020.119459

[29] PANZERA, T.H., CHRISTOFORO, A.L., RIBEIRO BORGES, P.H., "High performance fibre-reinforced concrete (FRC) for civil engineering applications", In: Bai, J. (ed), Woodhead Publishing Series in Civil and Structural Engineering, Advanced Fibre-Reinforced Polymer (FRP) Composites for Structural Applications, Sawston, Reino Unido. Woodhead Publishing, pp. 552–581, 2013. doi: http://dx.doi.org/10.1533/9780857098641.4.552

[30] BURATTI, N., FERRACUTI, B., SAVOIA, M., "Concrete crack reduction in tunnel linings by steel fibre-reinforced concretes", *Construction & Building Materials*, v. 33, pp. 249–259, 2013. doi: http://dx.doi.org/10.1016/j.conbuildmat.2013.02.063

[31] SUKONTASUKKUL, P., POMCHIENGPIN, W., SONGPIRIYAKIJ, S., "Post-crack (or post-peak) flexural response and toughness of fiber reinforced concrete after exposure to high temperature", *Construction & Building Materials*, v. 24, n. 10, pp. 1967–1974, 2010. doi: http://dx.doi.org/10.1016/j.conbuildmat.2010.04.003

[32] DÜLENCI, O., HAKTANIR, T., ALTUN, F., "Experimental research for the effect of high temperature on the mechanical properties of steel fiber-reinforced concrete", *Construction & Building Materials*, v. 75, pp. 82–88, 2014. doi: http://dx.doi.org/10.1016/j.conbuildmat.2014.11.005

[33] RAMASAMY, K., KANDASAMY, S., ANANDAKUMAR, S., *et al*., "Mechanical performance of hybrid engineered cementitious composites", *Cement, Wapno, Beton*, v. 24, pp. 479–486, 2019.

[34] DAI, Q., WANG, Z., MOHD HASAN, M.R., "Investigation of induction healing effects on electrically conductive asphalt mastic and asphalt concrete beams through fracture-healing tests", *Construction & Building Materials*, v. 49, pp. 729–737, 2008. doi: http://dx.doi.org/10.1016/j.conbuildmat.2013.08.089

[35] BEGLARIGALE, A., YAZICI, H., "Pull-out behavior of steel fiber embedded in flowable RPC and ordinary mortar", *Construction & Building Materials*, v. 75, pp. 255–265, 2014. doi: http://dx.doi.org/10.1016/j.conbuildmat.2014.11.037

[36] SÖYLEV, T.A., ÖZTURAN, T., "Durability, physical and mechanical properties of fiber-reinforced concretes at low-volume fraction", *Construction and Building Materials*, v. 73, pp. 67–75, 2009. doi: https://doi.org/10.1016/j.conbuildmat.2014.09.058

[37] ALTUN, F., HAKTANIR, T., ARI, K., "Effects of steel fiber addition on mechanical properties of concrete and RC beams", *Construction & Building Materials*, v. 21, n. 3, pp. 654–661, 2005. doi: http://dx.doi.org/10.1016/j.conbuildmat.2005.12.006

[38] ATIŞ, C.D., KARAHAN, O., "Properties of steel fiber reinforced fly ash concrete", *Construction & Building Materials*, v. 23, n. 1, pp. 392–399, 2007. doi: http://dx.doi.org/10.1016/j.conbuildmat.2007.11.002

[39] KAYALI, O., "Effect of high volume fly ash on mechanical properties of fiber reinforced concrete", *Materials and Structures*, v. 37, n. 269, pp. 318–327, 2004. doi: http://dx.doi.org/10.1617/13978

[40] MIRZA, F.A., SOROUSHIAN, P., "Effects of alkali-resistant glass fiber reinforcement on crack and temperature resistance of lightweight concrete", *Cement and Concrete Composites*, v. 24, n. 2, pp. 223–227, 2002. doi: http://dx.doi.org/10.1016/S0958-9465(01)00038-5

[41] ALI, M.A., MAJUMDAR, A.J., SINGH, B., "Properties of glass fibre cement — the effect of fibre length and content", *Journal of Materials Science*, v. 10, n. 10, pp. 1732–1740, 1975. doi: http://dx.doi.org/10.1007/BF00554935

[42] XIAOCHUN, Q., XIAOMING, L., XIAOPEI, C., "The applicability of alkaline-resistant glass fiber in cement mortar of road pavement: Corrosion mechanism and performance analysis", *International Journal of Pavement Research and Technology*, v. 10, n. 6, pp. 536–544, 2017. doi: http://dx.doi.org/10.1016/j.ijprt.2017.06.003

[43] MILLS, R.H., "Preferential precipitation of calcium hydroxide on alkali-resistant glass fibres", *Cement and Concrete Research*, v. 11, n. 5-6, pp. 689–697, 1981. doi: http://dx.doi.org/10.1016/0008-8846(81)90027-2

[44] PEREIRA-DE-OLIVEIRA, L.A., CASTRO-GOMES, J.P., NEPOMUCENO, M.C.S., "Effect of acrylic fibres geometry on physical, mechanical and durability properties of cement mortars", *Construction & Building Materials*, v. 27, n. 1, pp. 189–196, 2012. http://dx.doi.org/10.1016/j.conbuildmat.2011.07.061

[45] CAO, M., ZHANG, C., LV, H., "Mechanical response and shrinkage performance of cementitious composites with a new fiber hybridization", *Construction & Building Materials*, v. 57, pp. 45–52, 2014. doi: http://dx.doi.org/10.1016/j.conbuildmat.2014.01.088

[46] DIAMOND, S., "Effects of two Danish flyashes on alkali contents of pore solutions of cement-flyash pastes", *Cement and Concrete Research*, v. 11, n. 3, pp. 383–394, May 1981. doi: http://dx.doi.org/10.1016/0008-8846(81)90110-1

[47] MOREIRA, T.M., GENOVA, L.A., "Influência da composição e distribuição de tamanho de microesferas de Al_2O_3/Fe_2O_3, produzidas por gelificação interna, na adsorção de metais pesados", *Revista Matéria*, v. 28, n. 2, pp. e20230004, 2023. doi: https://doi.org/10.1590/1517-7076-RMAT-2023-0004